Population Ecology (2018) 60:9–20
https://doi.org/10.1007/s10144-018-0608-7

THE SOCIETY OF POPULATION ECOLOGY

SPECIAL FEATURE: ORIGINAL ARTICLE

Evolutionary demography: the dynamic and broad intersection of ecology and evolution

Size-dependent predation and correlated life history traits alter eco-evolutionary dynamics and selection for faster individual growth

John P. DeLong[1] · Thomas M. Luhring[1]

Received: 13 April 2017 / Accepted: 7 February 2018 / Published online: 5 March 2018

Abstract

Age at maturation is a key life history trait influencing individual fitness, population age structure, and ecological interactions. We investigated the evolution of age at maturity through changes in the von Bertalanffy growth constant for organisms with a simple juvenile-adult life history. We used Gillespie eco-evolutionary models to uncover the role of predation in driving the evolution of the growth constant when eco-evolutionary dynamics are present. We incorporated both size-independent and size-dependent predation into our models to generate differences in selection and dynamics in the system. Our results generally support the idea that faster ontogenetic growth is beneficial when populations are growing but that predation tends to have little effect on age at maturity unless there are trade-offs with other life history traits. In particular, if faster ontogenetic growth comes at the cost of fecundity, our results suggest that predation selects for intermediate levels of growth and fecundity. Eco-evolutionary dynamics influenced the nature of selection only when growth was linked to fecundity. We also found that predators that increasingly consume larger prey tend to have higher population sizes due to the greater energy intake from larger prey, but the growth rate-fecundity trade-off reversed this pattern. Overall, our results suggest an important role for interactions between size-dependent foraging and life-history trade-offs in generating varying selection on age at maturity through underlying growth traits.

Keywords Body size · Development time · GEM · Growth rate · Life history · Predation

Introduction

Age and size at maturity are key determinants of individual fitness (Reznick et al. 1990; Kozłowski 1992; Stearns 1992; Roff 1993; Darimont et al. 2009), and a fundamental trade-off underlies the point at which individuals make the juvenile-to-adult transition. Additional juvenile growth can lead to increased body size or fecundity that may increase fitness as adults, however, delaying maturation increases the risk of dying before reproducing. Thus, individuals should mature early and at a smaller size unless further growth confers additional benefits such as increased chance of survival or fecundity (Williams 1966; Gibbons et al. 1981; Roff 1986; Stearns 1992; Abrams and Rowe 1996; Luhring and Holdo 2015).

Predation is an important source of mortality risk for juveniles. Predation is expected to reduce age and size at maturity because it shifts the point at which the risk of mortality counteracts the gains of further growth (Abrams and Rowe 1996). This outcome is particularly noticeable in human-influenced systems such as fisheries (Ernande et al. 2004; Edeline et al. 2007; Darimont et al. 2009). Predators, however, may vary in the size of prey they select (Riessen 1999; Beckerman et al. 2010). Depending on the predator, then, organisms may be at more risk when they are small, due to the ease with which they may be captured, or when they are large, when they provide more energy to predators.

Evolution of life history traits such as age and size at maturity may occur quickly, on the order of a single to a few generations (Reznick et al. 1990; Darimont et al. 2009). These rapid shifts in traits may cause eco-evolutionary dynamics by changing the underlying ecological interactions

✉ John P. DeLong
jpdelong@unl.edu

[1] School of Biological Sciences, University of Nebraska, Lincoln, NE 68588, USA

(Hairston et al. 2005; Post and Palkovacs 2009; Schoener 2011; DeLong et al. 2016). Eco-evolutionary dynamics may play an important role in determining the outcome of selection on life history traits like age and size at maturity because the abundance of interacting species (e.g., predator and prey) may change, altering the strength or direction of selection as well as the availability of resources (Abrams and Rowe 1996; Edeline et al. 2007; Walsh and Reznick 2008; DeLong and Walsh 2016). Furthermore, selection itself may reduce heritable trait variation in life history traits, limiting the potential for further responses to selection over time (Wright 1931, 1949). It is thus crucial to consider the role of eco-evolutionary dynamics when trying to understand the role of predation in driving the evolution of age and size at maturity.

For many organisms, individual growth can be described by the von Bertalanffy growth model, $m = m_\infty\left(1 - e^{(-k_{\text{vb}}t)}\right)$, where m is body size at time t, m_∞ is the asymptotic size, and k_{vb} is the growth constant, or rate at which the asymptotic size is approached (von Bertalanffy 1960). Size at maturity (m_α) is defined as the size reached at the age at maturity (α):

$$m_\alpha = m_\infty\left(1 - e^{(-k_{\text{vb}}\alpha)}\right). \quad (1)$$

Solving Eq. 1 for α, we see that maturity can also be described as the time when some fraction (f_{sam}) of the asymptotic size is reached:

$$\alpha = \frac{\ln\left(1 - \frac{m_\alpha}{m_\infty}\right)}{-k_{\text{vb}}} = \frac{\ln\left(1 - f_{\text{sam}}\right)}{-k_{\text{vb}}}. \quad (2)$$

For individuals growing according to the von Bertalanffy growth model, earlier maturity can be achieved by increasing the growth constant (Fig. 1a), lowering the size at maturity, or equivalently lowering f_{sam}, or finally increasing the asymptotic size. These three traits (k_{vb}, m_∞, f_{sam}) may be under selection due to their effects on age at maturity, and we therefore focus on the evolution of the underlying traits rather than size or age at maturity itself.

Here we use a new approach for modeling eco-evolutionary dynamics known as Gillespie eco-evolutionary models (GEMs) to investigate the effect of predation risk on the evolution of von Bertalanffy growth parameters (DeLong and Gibert 2016). We initially assessed the effects of predation on age of maturation through all three parameters (k_{vb}, m_∞, f_{sam}), but since the results were similar, we focus here on the role of k_{vb} for brevity. Because it is in the denominator of Eq. 2, increasing k_{vb} has an inverse effect on the age of maturation, such that when small, increasing k_{vb} can reduce time to maturation considerably, but when larger, very little additional change in the timing of maturation can be achieved (Fig. 1b). We explored how predation affects the evolution of k_{vb} by examining trait and population dynamics with and without predators and with variation in the size-dependency of predation. We also incorporated trade-offs through commonly seen negative relationships between k_{vb} and other life history traits (asymptotic size and fecundity) to determine whether the costs of faster individual growth influence selection on k_{vb}.

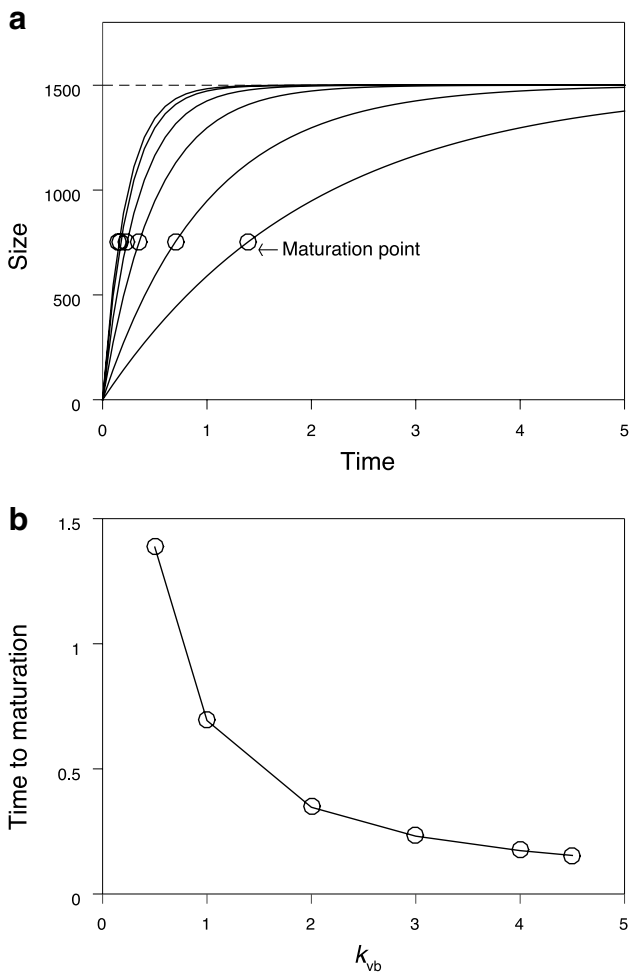

Fig. 1 Von Bertalanffy growth curves. **a** Increasing k_{vb} causes size to increase toward asymptotic size (dashed line) more quickly, thus reaching maturation (circles) more quickly. Lines decrease in k_{vb} from left to right. **b** The effect of k_{vb} on time to maturation is non-linear, becoming a less effective way of maturing faster as it increases, given a fixed asymptotic size and size fraction of maturity

Methods

The model

We modified the MacArthur-Rosenzweig predator–prey model (Rosenzweig and MacArthur 1963) to accommodate

a prey species that has a simple age structure of juveniles (J) and adults (A):

$$\frac{dJ}{dt} = fA - \frac{J}{t_{2\alpha}} - \frac{fJ(J+A)}{K} - \frac{aJP}{1+ahJ} \tag{3a}$$

$$\frac{dA}{dt} = \frac{J}{t_{2\alpha}} - \frac{fA(J+A)}{K} - \frac{aAP}{1+ahA} \tag{3b}$$

$$\frac{dP}{dt} = \frac{e_a aAP}{1+ahA} + \frac{e_j aJP}{1+ahJ} - dP \tag{3c}$$

In this model, f is adult prey fecundity and K is prey carrying capacity. The density-dependent effect of the logistic model is separated into its effects on juvenile and adult mortality ($\frac{fJ(J+A)}{K}$ and $\frac{fA(J+A)}{K}$, respectively). In addition, a is the space clearance rate for the predator's functional response, h is handling time, e is the conversion efficiency for turning prey into new predators, d is predator background death rate, and $t_{2\alpha}$ is the time remaining to adulthood. We use separate conversion efficiencies for juveniles (e_j) and adults (e_a), as due to their larger size, adults provide more energetic benefit to the predators. These are calculated as GGE × prey size/predator size, where GGE is the gross growth efficiency.

The maturation rate of juveniles into adults is given by the inverse of the time remaining to adulthood ($t_{2\alpha}$), which is the difference between α (age at maturation) and the current age (t_c). We substituted t_c for α and m_c (current body size) for m_α in Eq. 2 to get $t_c = \frac{\ln\left(1-\frac{m_c}{m_\infty}\right)}{-k_{vb}}$, which we combine with Eq. 2 to get the time it takes for an individual to grow from its current size to its maturation size:

$$t_{2\alpha} = \alpha - t_c = \frac{\ln\left(1-\frac{m_c}{m_\infty}\right) - \ln\left(1-f_{sam}\right)}{k_{vb}} \tag{4}$$

We use Eq. 3a, 3b, 3c to understand the evolution of the von Bertalanffy growth constant k_{vb}. Note that as $t_{2\alpha} \to 0$, Eq. 3a, 3b, 3c converges back to a standard MarArthur-Rosenzweig model (Fig. 2).

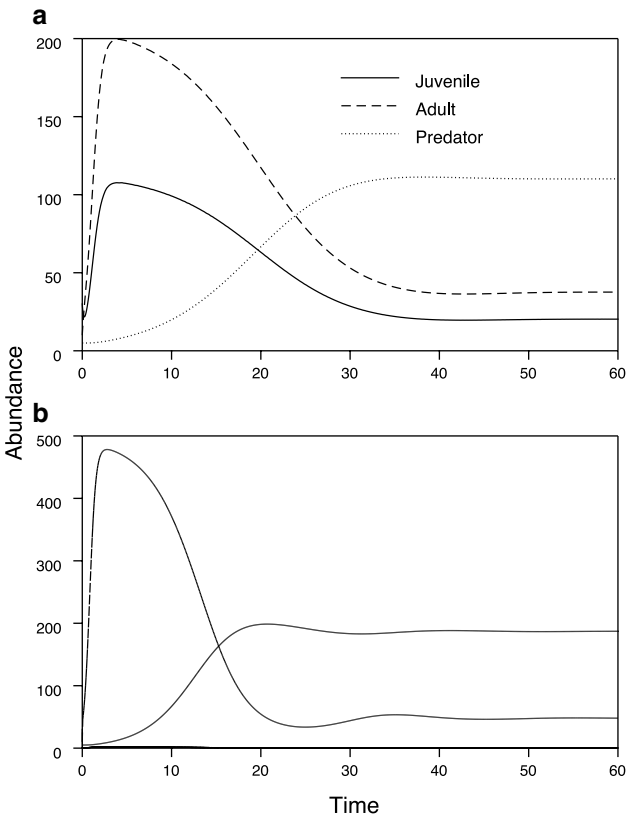

Fig. 2 Solutions of our modified MacArthur-Rosenzweig (MR) model to include a simple juvenile/adult age structure. The model reduces to the MR model when the maturation time becomes very small. The addition of a juvenile and adult class to the model has a tendency to dampen the oscillations that often occur in the MR model. **a** Example dynamics with $k_{vb} = 2.5$, $e_j \approx 0.01$, $e_a = 0.06$, $K = 500$ ind mL^{-1}, $d = 0.042$ d^{-1}, $h = 0.02$ d, $f_{sam} = 0.5$, and the functional response is as reported in the text. Starting population sizes were 5 predators and 40 prey. **b** When k_{vb} becomes very large, juveniles instantaneously become adults, making the juvenile curve go to zero abundance. Other parameters are the same as in **a**

How GEMs work

GEMs work by breaking down the rates in an ordinary differential equation (ODE) model into discrete events whose probability depends on the relative magnitude of the rate term, as in a standard Gillespie simulation (Yaari et al. 2012; DeLong and Gibert 2016). GEMs make the simulation evolutionary by representing populations with distributions of traits that influence the rate parameters and thus the likelihood of events. Any trait that increases the likelihood of a birth or decreases the likelihood of a death will be favored in the population because similar individuals will be added upon a birth (as a function of the trait's heritability, see below) or removed from the population, respectively, causing the trait distribution to move toward higher fitness values. Thus, GEMs function as a computational analog to natural selection in real populations by allowing trait distributions to move in response to individual-level differences in fitness. The ODE model itself creates the fitness landscape that drives evolution, and because the system changes through time, the fitness landscape changes through time as well. GEMs allow traits to evolve alongside the ecological dynamics, generating eco-evolutionary dynamics.

The GEM algorithm begins by seeding a population with an initial trait distribution (Fig. 3). Then, an individual is chosen at random from the distribution, and model terms are calculated given the effect of the trait on model parameters. An event (i.e., birth, death, predation, maturation; Table 1) is then chosen wheel-of-fortune style, where larger terms are

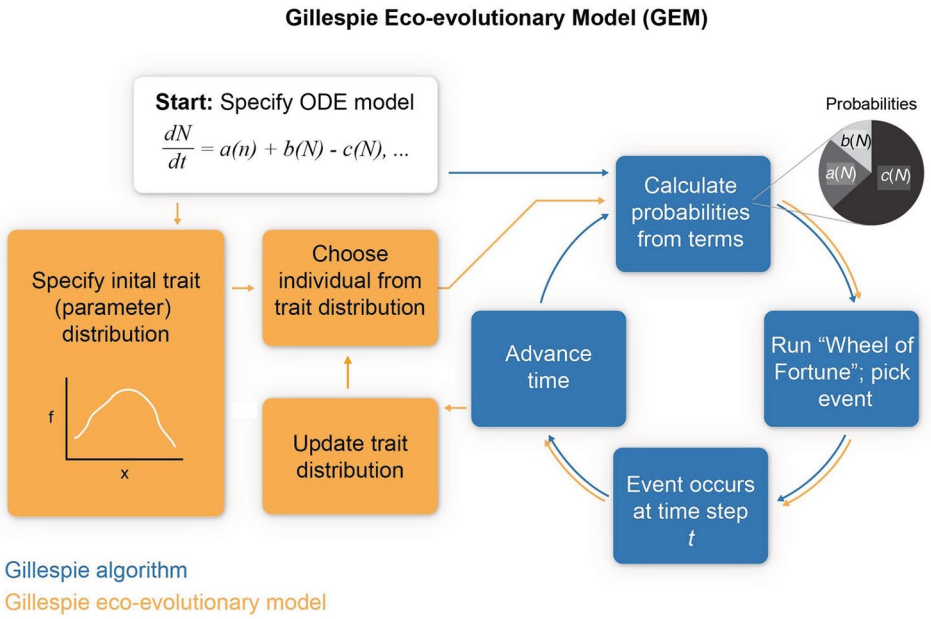

Fig. 3 A schematic of how Gillespie eco-evolutionary models (GEMs) operate. See main text for description. Reproduced from DeLong and Gibert 2016

Table 1 Possible events that can occur in Eq. 3a, 3b, 3c, separated out for the events that can occur when a juvenile versus an adult is chosen

Event	Juveniles	Adults
Reproduction		X
Maturation	X	
Death by density dependence	X	X
Death by predation	X	X
Predator birth	X	X
Predator death	X	X

more likely to be chosen because they represent larger areas on the wheel-of-fortune. Then the event transpires by adding or substracting an individual to the population. If an individual is added to the population, it is given a trait following the rules of heritability (see below). Time then advances in steps randomly drawn from an exponential distribution, a new individual is drawn, and the cycle continues.

Advantages of GEMs for understanding eco-evolutionary dynamics over other modeling approaches include that (1) heritable trait variance is both tracked and updated in real time, allowing changes in variance to influence further selection, (2) assumptions about fitness gradients are generated by the model itself rather than by a priori assumptions about how fitness is maximized, and (3) fitness gradients change through time and thus naturally capture changes in context and potential indirect effects.

Events for adults and juveniles

In this GEM, we do not track predator traits, so predator births and deaths simply add or subtract an individual from the predator population. In contrast, prey births and deaths influence the trait distribution. We define age-specific events and probabilities separately for juveniles and adults because not all events can occur for each age class (Table 1). Time advances after each event, but before the cycle continues, all individuals are allowed to grow given the time step (t_s) and their individual growth curve:

$$m_{c+t_s} = m_\infty \left(1 - e^{\left[\ln\left(1-\frac{m_c}{m_\infty}\right) - k_{vb} t_s\right]}\right). \quad (5)$$

In this GEM, prey have three traits—a current size (m_c), a growth constant (k_{vb}), and an asymptotic size (m_∞). When initiating populations and generating offspring in the simulations, the growth constant is chosen first, and a current size is then generated by calculating a random fraction of the asymptotic size. Thus, whenever an individual is chosen for an event, it has three traits that determine its maturation time and further growth (m_c, k_{vb}, and m_∞) and one trait that determines its size-dependent interaction with a predator (m_c).

Designation of offspring traits

New offspring are assigned a k_{vb} by randomly drawing it from a distribution of potential k_{vb} that depend on the parent's trait (p), the heritability of that trait (h^2), and the level of trait variation in the population. Here we use o for offspring trait because the designation can be used for any trait, not just k_{vb}. The distribution from which the trait is drawn has a mean of the expected value of the offspring trait, $E[o]$, that is determined by a parent-offspring regression. The expected value is calculated in the following way: In a parent-offspring regression, narrow-sense heritability h^2

is the slope of the line relating parent (p) and offspring (o) traits. The intercept of this line is 0 when $h^2 = 1$, but when $h^2 < 1$, the intercept can be found by solving for it given that the overall mean offspring $\bar{o}$ and mean parent traits $\bar{p}$ are equal, giving the expected value of the current offspring's trait as $E[o_c] = h^2 p_c + \bar{p}(1 - h^2)$, where p_c is the current parent's trait.

We assign a level of variance around the expected value of the offspring trait using an estimator of the explained variance (R^2) of the parent-offspring regression. We do this because the parents' traits explain some portion of the offspring traits, while the noise around the regression line is the unexplained variance, or $1 - R^2$. Because the actual parent-offspring regression is here unknown, we estimate R^2 from h^2 in several steps. First, the slope of the parent-offspring regression is calculated as $h^2 = \frac{cov(o,p)}{\sigma_p^2}$. Thus, knowing the h^2 and the variance in p, we can estimate the covariance between o and p as $cov(o,p) = \sigma_p^2 h^2$. The R^2 of a parent-offspring regression is equal to the square of the correlation coefficient, or $R^2 = \left(\frac{cov(o,p)}{\sigma_o \sigma_p}\right)^2 = \frac{cov(o,p)^2}{\sigma_o^2 \sigma_p^2}$. In a parent-offspring regression, it is also expected that the variance in offspring and parent traits is approximately equal, thus $R^2 = \frac{(h^2)^2 (\sigma_p^2)^2}{(\sigma_p^2)^2} = (h^2)^2$, and so the unexplained noise (ν) around the expected value of the offspring trait has a standard deviation of $\nu_{\sigma o} = \sigma_p \sqrt{1 - (h^2)^2}$. We use the heritability-weighted mean of the initial and current population variance to estimate the current σ_p, because estimates of current standing variation cause rapid, stochastic loss of genetic variance through time. We therefore randomly draw offspring traits from a lognormal distribution with mean $E[o_c]$ and standard deviation $\nu_{\sigma o}$.

Parameterization

We initiated prey populations of 40 individuals with a trait distribution with a mean k_{vb} of 2.5 and a coefficient of variation of 0.2 (a reasonable level of heritable trait variation; Lande 1977). A current size was assigned to each individual as a random fraction of asymptotic size (see below). We set f_{sam} at 0.5 and assigned age class depending on whether the current size was below (juvenile) or above (adult) $f_{sam} \times m_\infty$. Thus the initial number of juveniles and adults in the population varies from run to run. Because we found similar results after using a range of f_{sam} values (0.25–0.75), we used $f_{sam} = 0.5$ for the results reported here.

For body size, functional response, carrying capacity, and mortality rates, we used values typical for heterotrophic protists because the body size dependence of consumer-resource model parameters are well worked out for these organisms (DeLong et al. 2015). We set adult prey asymptotic size at 1.5×10^3 μm^3 and predator size at 1×10^4 μm^3. We set GGE at 0.4 (Rogerson 1981). Using the prey asymptotic size, this gives a conversion efficiency for predators consuming adults of $e_a = 0.06$. The conversion efficiency for predators consuming juveniles varies from run to run given the observed per-simulation initial mean juvenile size but is about $e_j \approx 0.01$. Handling time was set at 0.02 d, predator death rate at 0.042 d^{-1}, and carrying capacity at 500 ind mL^{-1}.

We calculated the functional response parameter a (space clearance rate) allometrically from prey size. We did this by first assessing the effect of prey body size on space clearance rate with linear models where the logs of predator and prey body size are predictor variables and the log of space clearance rate was the response variables, using the cross-species protist dataset from DeLong et al. (2015). This yielded a power-law function for space clearance rate: $a = 0.0034 \times V^{0.2}$, where V is prey cell volume in μm^3. The size-independent a was calculated from this equation using the initial mean prey volume. Positive size-dependent foraging was added simply by calculating a new a for each individual for each event given the current prey size (m_c) using $a = 0.0034 \times m_c^{0.2}$. Although empirically we know that space clearance rate increases with prey size in protists, we also reversed the sign of the exponent of the power law to explore the potential for negative size-dependence. To do this, we calculated a new intercept such that the space clearance rate at the mean starting prey body size is equal in both treatments and is equal to the overall space clearance rate parameter in the size-independent foraging version. The equation for negative size-dependent foraging is thus $a = 0.037 \times V^{-0.2}$.

Simulations

We ran the GEM in four sets of simulations (all with 200 replicate runs) of increasing complexity, from no predators, to predators with size-dependent foraging, to two scenarios where trade-offs create costs to increasing k_{vb}. These two trade-off scenarios reflect relationships that can be seen empirically for some species and thus are reasonable cost functions to include (Charnov 1993; Berrigan and Charnov 1994; Perrin 1995; DeLong and Hanley 2013): (1) In the first set of simulations, we ran the GEM without predators by initiating predator populations with 0 individuals. In this analysis, selection on k_{vb} occurs strictly through the fitness consequences of earlier maturation with no influence from predation. (2) In the second set of simulations, we introduced predators at an initial population size of five and compared outcomes from the three types of size-dependent predation (increasing with prey size, decreasing with prey size, and independent of prey size). (3) In the third set of simulations, we introduced a cost function that would work against selection on k_{vb}. We linked m_∞ to k_{vb} using a trade-off that

takes resource supply as a constraint (DeLong 2012). In this model, asymptotic size is linked to overall supply (S) and resource demand, such that asymptotic size is a function of the inverse of demand, which in this case is generated by changes in the growth constant:

$$m_{\infty} = \left(\frac{S}{k_{\mathrm{vb}}}\right)^{1/b}. \quad (6)$$

In Eq. 6, b is the exponent of the relationship between metabolic demand and body size, which we assume is 0.75. We also assume that the resource supply is sufficient to cover resource needs at the mean expected m_{∞}, so $S = k_{\mathrm{vb}} \times m_{\infty}^{0.75}$. (4) In the fourth set of simulations, we introduced a different cost function that would work against selection on k_{vb}. In this cost function, f is linked to k_{vb}, reflecting a trade-off between allocation to growth versus offspring (Edeline et al. 2007; Folkvord et al. 2014; Audzijonyte and Kuparinen 2016). We modeled this trade-off with an inverse function where the mean k_{vb} corresponds to an overall mean value for m_{∞} of 1.5×10^3 μm^3. We first show the cost effect for the different size-dependent foraging relationships. We then vary the starting value of k_{vb} (from 0.5 to 4.5) for positive size-dependent foraging to illustrate the effect of changing initial conditions on the eco-evolutionary dynamics.

Results

Simulation section 1

Without predators, the prey evolved faster growth rates while the prey population was expanding, but no further evolution of k_{vb} occurred after populations stabilized (Fig. 4). This was true even if lower values of k_{vb} were used that might create a stronger selection differential on k_{vb}. In addition, when there were no predators, the prey populations grew to a stable population size with a stable age distribution.

Simulation section 2

When predators were added, a similar pattern of evolution toward faster growth occurred regardless of how prey size

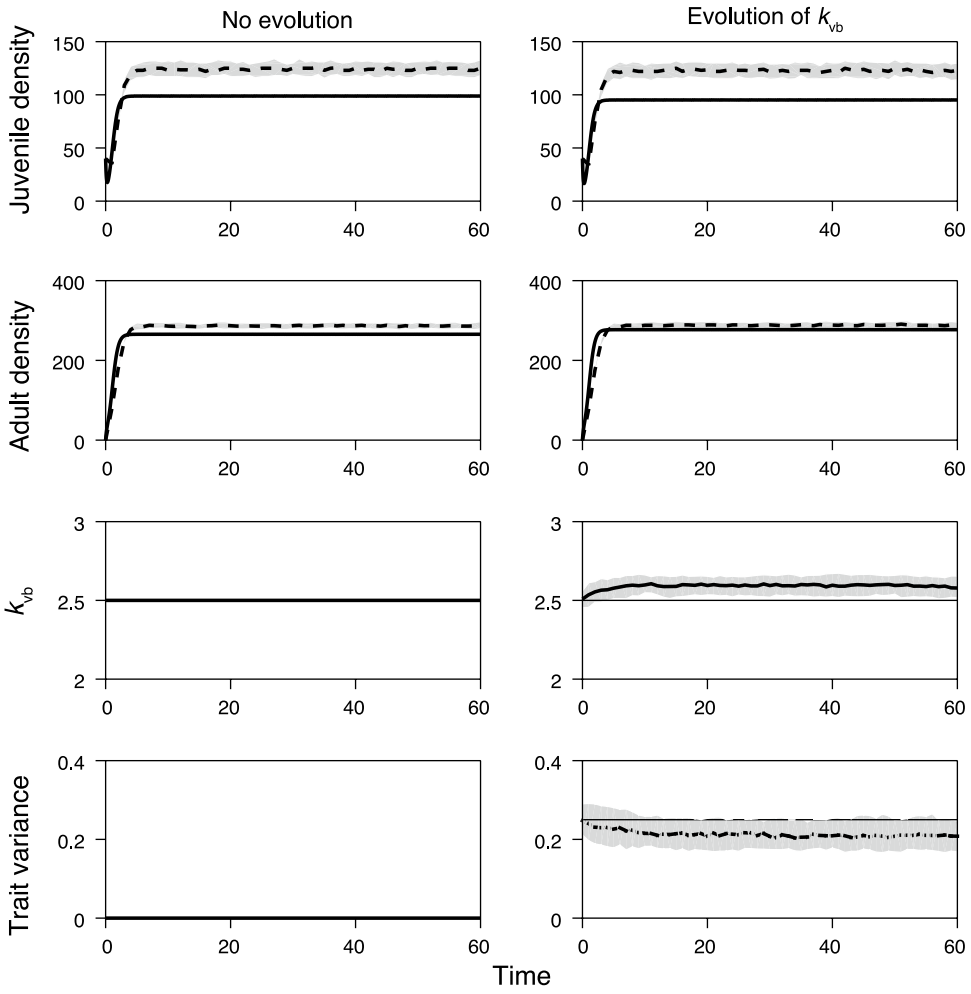

Fig. 4 Evolution of the von Bertalanffy growth constant k_{vb} in a predator-free model. Left column shows a no-evolution scenario generated by reducing trait variance to zero. The right column shows the evolution scenario. In both scenarios, juvenile and adult populations increase and stabilize, with some transient dynamics evident. In the evolution scenario, k_{vb} (third row of plots) evolves toward higher values (resulting in faster attainment of maturity) during the growth phase and then oscillates randomly. Trait variation remains zero in the no-evolution scenario but in the evolution scenario is maintained close to original levels despite selection on k_{vb}. Solid black lines show the solution from a standard ODE solver with no evolution, the dashed black lines show the median GEM solution, and the shaded gray regions show the middle 50% of the GEM solutions

was linked to foraging in the predator (Fig. 5). That is, k_{vb} increased only during the prey's growth phase, and growth of the predator population had little effect on further evolution of k_{vb} in the absence of trade-offs.

Despite the consistency of evolution toward faster k_{vb}, the eco-evolutionary dynamics differed depending on the size-dependence of foraging (Fig. 5). The ecological dynamics of the size-independent foraging were indistinguishable from the no-evolution scenarios. When foraging increased with prey size, predators grew faster and lowered both young and adult abundances relative to the no-evolution simulations at steady state, while the opposite was true when foraging decreased with prey size. This outcome arises because adults provide greater energetic

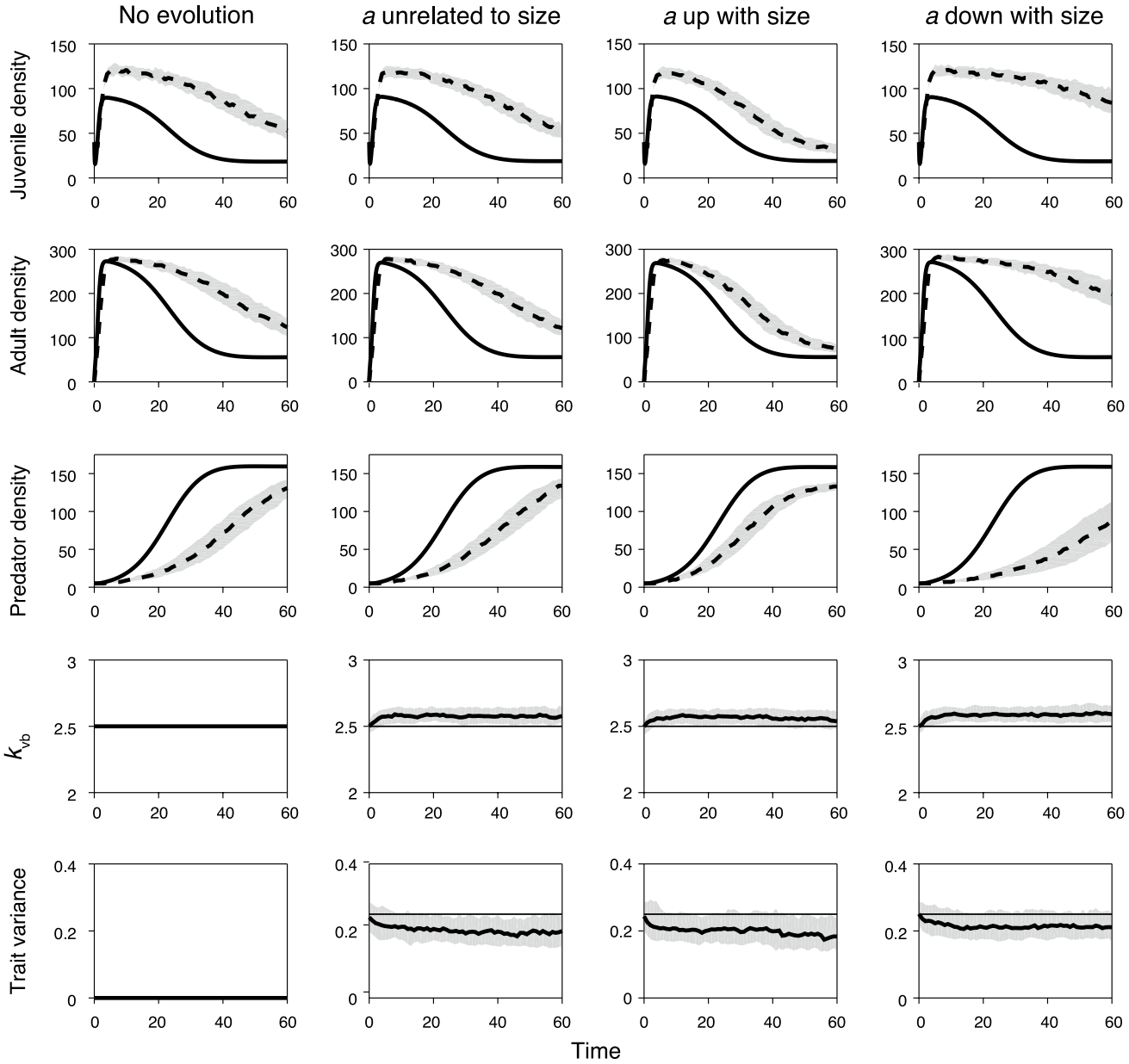

Fig. 5 Evolution of the von Bertalanffy growth constant k_{vb} under predation risk, when k_{vb} is not linked to other life history traits. The left column shows the no-evolution scenario, and the other columns show the effect of size-independent predation (second column), predation increasing on larger-sized prey (third column), and predation increasing on smaller-sized prey (fourth column). All simulations show growth of both juvenile (top row) and adult (second row) populations followed by population reductions due to predators (third row). Solid black lines show the solution from a standard ODE solver with no evolution, the dashed black lines show the median GEM solution, and the shaded gray regions show the middle 50% of the GEM solutions. All evolution scenarios show evolution toward faster growth (fourth row) accompanied by some loss of trait variance (fifth row). Size dependent foraging generates opposing effects on eco-evolutionary dynamics, which are detectable as differences in the curves between the evolution and no-evolution panels

yield, allowing the predators to grow faster when foraging on a higher proportion of adults.

Simulation section 3

Different outcomes arose when k_{vb} was connected to other parameters (i.e., when trade-offs were present). When connected to m_{∞}, k_{vb} evolved to be slightly faster than it did independently (Fig. 6). The eco-evolutionary dynamics were otherwise similar to the results without a link between k_{vb} and m_{∞}.

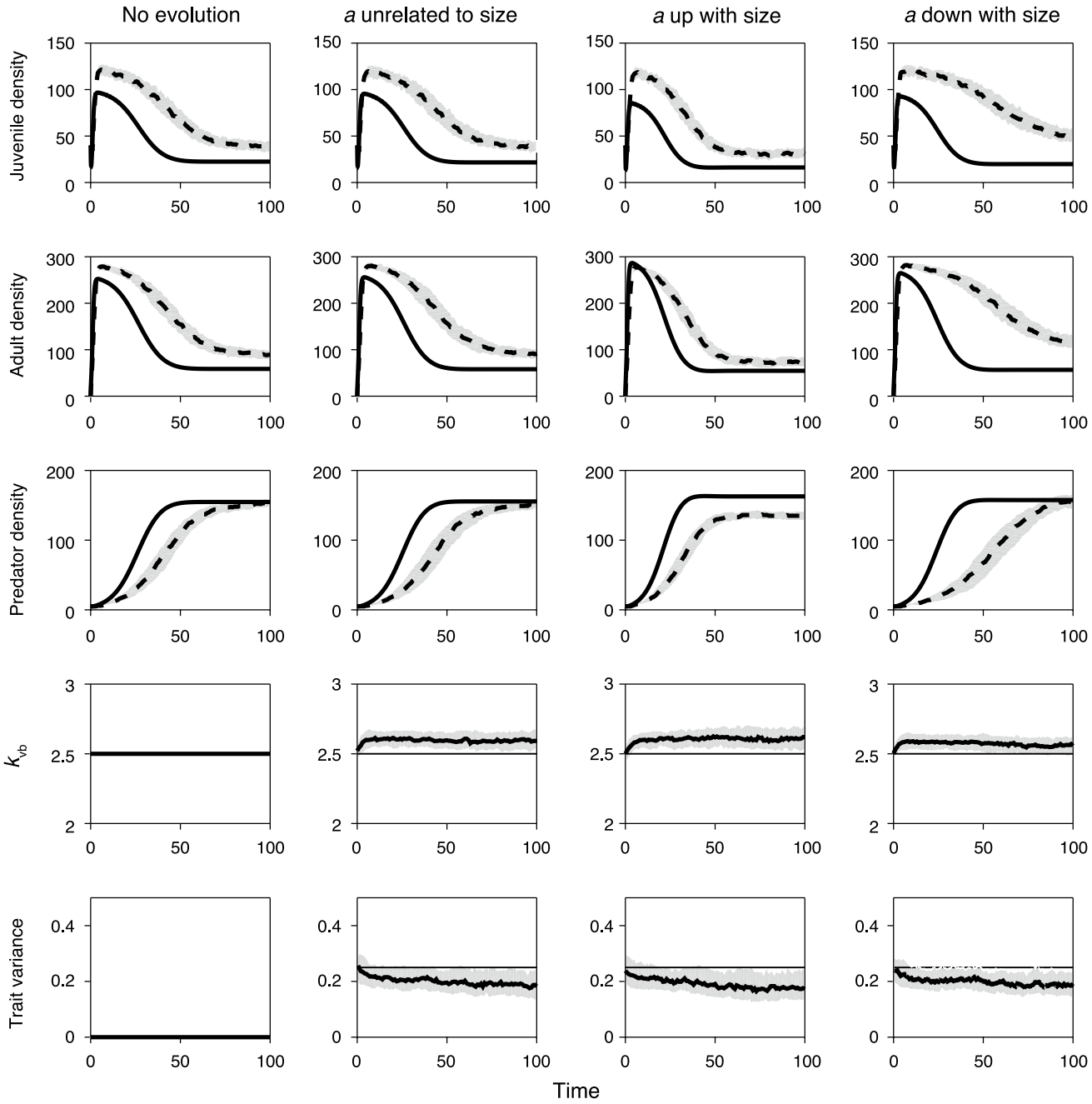

Fig. 6 Evolution of the von Bertalanffy growth constant k_{vb} under predation risk when it is negatively correlated with asymptotic size. Panel arrangement by rows and columns follows Fig. 5. Solid black lines show the solution from a standard ODE solver with no evolution, the dashed black lines show the median GEM solution, and the shaded gray regions show the middle 50% of the GEM solutions. Outcomes for traits and dynamics are very similar to results with independent k_{vb} (Fig. 5), but the correlation with asymptotic size leads to slightly higher growth rate values

Simulation section 4

When connected to fecundity, there was evolution toward higher k_{vb} during the initial prey growth period, but the selection reversed as the predator population grew, moving k_{vb} back toward, and in some cases even lower than, its original values (Fig. 7). The eco-evolutionary dynamics were similar between the correlated trait and single trait simulations (Fig. 6 versus Fig. 7), but with slightly more exaggerated differences in predator abundance in the size-dependent foraging versions. Finally, the pattern of k_{vb} evolution changed as the initial value of k_{vb} increased (Fig. 8). When k_{vb} was low, there was positive selection that increased k_{vb} by about 20% above its original value

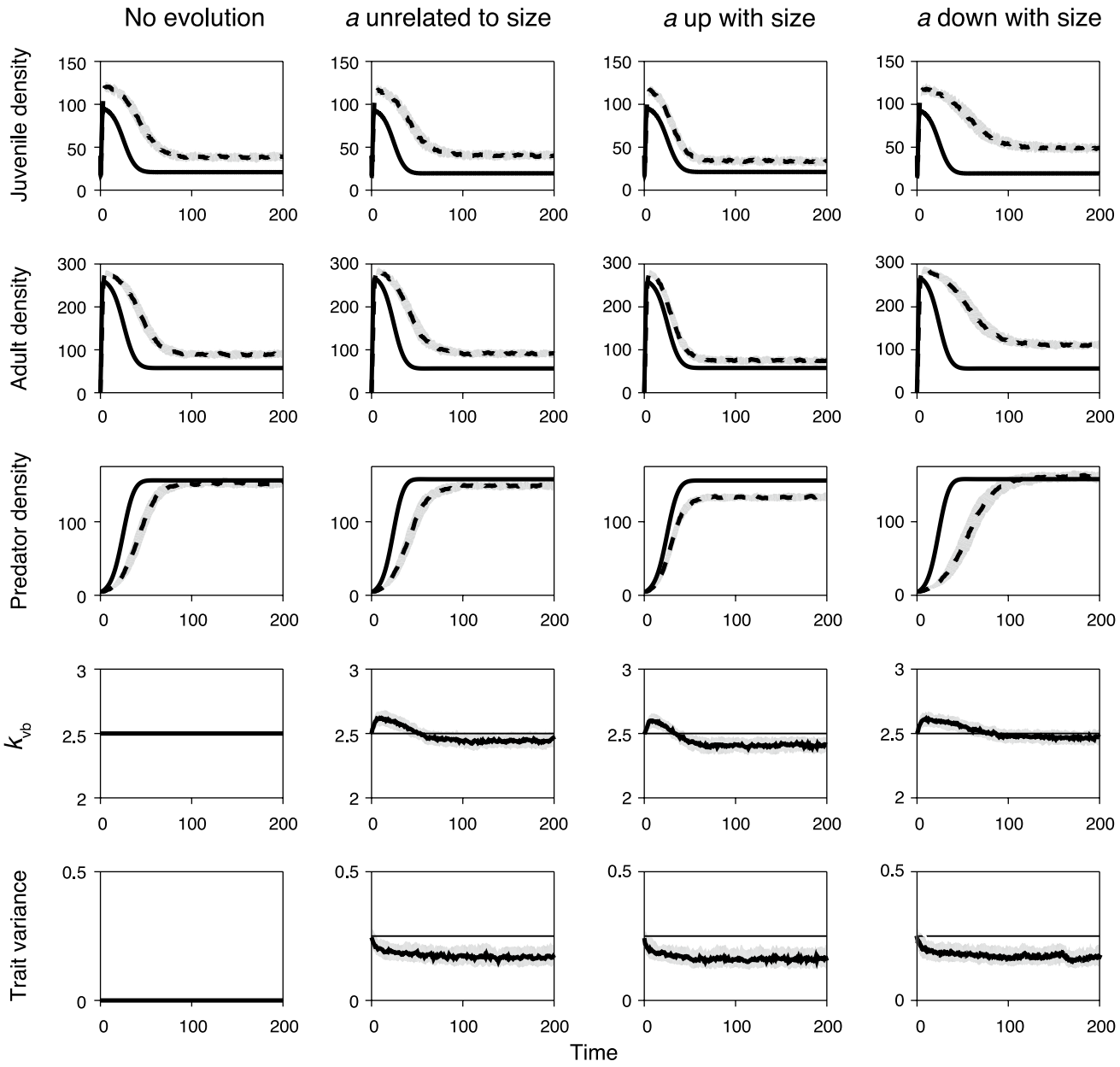

Fig. 7 Evolution of the von Bertalanffy growth constant k_{vb} under predation risk when is negatively correlated with fecundity. Panel arrangement by rows and columns follows Fig. 5. Solid black lines show the solution from a standard ODE solver with no evolution, the dashed black lines show the median GEM solution, and the shaded gray regions show the middle 50% of the GEM solutions. Outcomes are similar to results with independent k_{vb} (Fig. 5) but are drawn to much longer time frames to see the long-term effects. The correlation with fecundity appears to not alter selection toward higher growth rate values during the prey growth period, but it does reverse selection over the long term (row 4). The time scale and magnitude of this reversal depends on the nature of size-selective predation

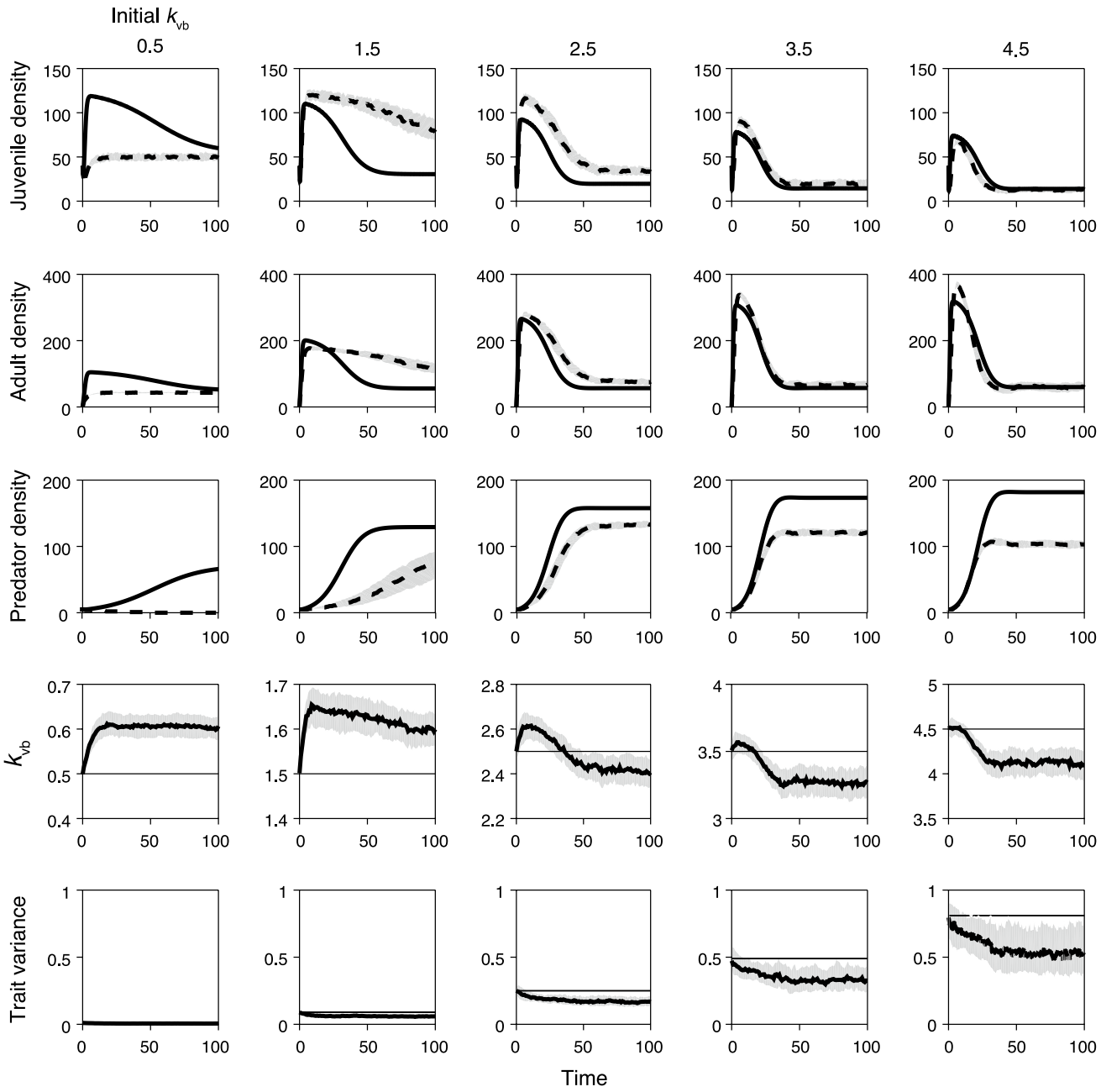

Fig. 8 Evolution of the von Bertalanffy growth constant k_{vb} under predation risk when it is negatively correlated with fecundity and with positive prey size selection. Here we show the same conditions as in Fig. 7, column 3, but with a range of initial k_{vb} values (increasing from left to right across columns). In all cases, selection for higher k_{vb} is halted or reversed, with the eventual trait value increasing with the starting value. As k_{vb} increases, the growth of individuals and movement of juveniles to adults occurs more quickly, lowering juvenile abundance. The increased production of adults also increases predator density because predators are choosing larger prey, but selection against high k_{vb} values limits this effect. Solid black lines show the solution from a standard ODE solver with no evolution, the dashed black lines show the median GEM solution, and the shaded gray regions show the middle 50% of the GEM solutions

but with no eventual reversal, whereas when k_{vb} was high, there was no period of positive selection and only negative selection that decreased k_{vb} by about 10%.

Discussion

The role of predation (or harvesting) in driving evolution of earlier maturation (lower age at first reproduction) is a key issue for evolutionary theory and the management of economically important resources (Stearns et al. 2000;

Conover and Munch 2002; Ernande et al. 2004; Kozłowski et al. 2004; Darimont et al. 2009). We investigated the evolution of age at maturity by focusing on a key underlying trait that determines this age—the von Bertalanffy growth constant. Our findings suggest that faster k_{vb} is beneficial during periods of rapid population growth (Figs. 4, 5, 6, 7, 8), consistent with compound-interest theory (Lewontin 1965). This suggests that the primary driver of faster k_{vb} in our results is not predators *per se* but the advantage of earlier reproduction during exponential growth phases. This type of response has been seen empirically, for example along wave fronts of invading cane toads (Phillips et al. 2010) or among rapidly growing aphid populations (Turcotte et al. 2011).

Unexpectedly, our findings suggest little role for predation in driving faster growth rates. In all simulations, k_{vb} stopped changing when prey populations stopped growing and predator populations started increasing. This was true regardless of whether predation was size independent or changed with prey size. The lack of change in k_{vb} after the prey population growth period cannot be explained by an excess loss of variance, as variance eroded only slightly during the evolutionary period and was maintained at relatively high levels throughout the remainder of all simulations. It is thus more likely that the fitness benefits of earlier maturation under predation are limited when a population is no longer growing. When a trade-off between individual growth rate and fecundity was assumed, there is still rapid evolution of higher k_{vb} during prey population growth phases. When the predator population started growing, however, evolution of k_{vb} reversed, returning this trait back toward starting values (Fig. 7). This lower k_{vb}, however, is rewarded with higher fecundity, indicating that the fitness benefit of higher fecundity outweighs that of earlier maturation during periods of heavy predation. This outcome was foreshadowed by Abrams and Rowe (1996), who indicated that stable populations under predation risk should experience selection towards higher reproductive output, whereas growing populations would experience the opposite. This pattern, however, depended on the nature of predation, with the reversal and suppression of k_{vb} being fastest and furthest when predation was stronger on larger individuals.

In contrast to the above example, when k_{vb} was negatively correlated with m_{∞} (i.e., fast growth leads to small maximum size), we found that k_{vb} evolved to be slightly higher than it did independently. This result is somewhat paradoxical, because the negative relationship between k_{vb} and m_{∞} is generally thought of as a trade-off, perhaps caused by a constraint, where an organism cannot both grow fast and support a large body at the same time (Charnov 1993; Perrin 1995; DeLong 2012). However, the negative correlation means that both fast growth and a reduced asymptotic size result in earlier maturation. In other words, the fitness advantage of faster growth is further boosted by arriving at the asymptotic size earlier. So in this case, a trade-off creating a negative relationship between growth rate and maximum adult size actually becomes a trait suite favoring fast maturation on one end of the spectrum and slow maturation on the other end.

Our use of GEMs allowed us to uncover unexpected aspects of the selection on k_{vb} under predation risk. In part this is due to the incorporation of eco-evolutionary dynamics and shifts in the nature of selection through time. For example, we observed selection for faster k_{vb} only until predation halted the prey's population growth, at which point selection for higher fecundity occurred, at least where k_{vb} was initially very low. The trade-off that facilitated a reverse in selection also reversed patterns of eco-evolutionary dynamics. When k_{vb} evolved independently or in connection with asymptotic size (Figs. 5, 6), predator populations grew to higher levels when they foraged more intensively on larger prey than when they foraged more intensively on smaller prey. This outcome arises due to the increased energetic yield of larger prey. However, when the trade-off between growth and fecundity was included (Fig. 7), this pattern was reversed, potentially because the increased fecundity and slower growth boosted the juvenile population and allowed predation rates to increase.

GEMs are inherently a form of evolutionary demography, linking traits directly to vital rates (birth, death, growth, maturation) and ecological interactions central to births and deaths (e.g., predation). By incorporating the effect of traits on event likelihoods, GEMs allow us to simulate ODE solutions where traits can evolve and the consequences of that evolution (changes in both the mean and variance of those traits) immediately feed back into the dynamics. In this way, GEMs provide a computational analog to natural selection and generate eco-evolutionary dynamics in response to evolution. GEMs capture changes in the strength and direction of selection because fitness gradients are dynamic and arise from the structure of the model and the changing abundances and traits that drive demographic processes.

Acknowledgements Support for this work was provided by BSF grant # 2014295 (JPD), a McDonnell Foundation complex systems scholar award (JPD), and the University of Nebraska Program of Excellence in Population Biology post-doctoral fellowship to TML.

References

Abrams PA, Rowe L (1996) The effects of predation on the age and size of maturity of prey. Evolution 50:1052–1061

Audzijonyte A, Kuparinen A (2016) The role of life histories and trophic interactions in population recovery. Cons Biol 30:734–743

Beckerman AP, Rodgers GM, Dennis SR (2010) The reaction norm of size and age at maturity under multiple predator risk. J Anim Ecol 79:1069–1076

Berrigan D, Charnov EL (1994) Reaction norms for age and size at maturity in response to temperature: a puzzle for life historians. Oikos 70:474–478

Charnov EL (1993) Life history invariants: some explorations of symmetry in evolutionary ecology. Oxford University Press, Oxford

Conover DO, Munch SB (2002) Sustaining fisheries yields over evolutionary time scales. Science 297:94–96

Darimont CT, Carlson SM, Kinnison MT, Paquet PC, Reimchen TE, Wilmers CC (2009) Human predators outpace other agents of trait change in the wild. Proc Natl Acad Sci USA 106:952–954

DeLong JP (2012) Experimental demonstration of a 'rate-size' tradeoff governing body size optimization. Evol Ecol Res 14:343–352

DeLong JP, Gibert JP (2016) Gillespie eco-evolutionary models (GEMs) reveal the role of heritable trait variation in eco-evolutionary dynamics. Ecol Evol 6:935–945

DeLong JP, Hanley TC (2013) The rate-size trade-off structures intraspecific variation in *Daphnia ambigua* life history parameters. PLoS One 8:e81024

DeLong JP, Walsh MR (2016) The interplay between resource supply and demand determines the influence of predation on prey body size. Can J Fish Aquat Sci 73:709–715

DeLong JP, Gilbert B, Shurin JB, Savage VM, Barton BT, Clements CF, Dell AI, Greig HS, Harley CDG, Kratina P, McCann KS, Tunney TD, Vasseur DA, O'Connor MI (2015) The body size dependence of trophic cascades. Am Nat 185:354–366

DeLong JP, Forbes VE, Galic N, Gibert JP, Laport RG, Phillips JS, Vavra JM (2016) How fast is fast? Eco-evolutionary dynamics and rates of change in populations and phenotypes. Ecol Evol 6:573–581

Edeline E, Carlson SM, Stige LC, Winfield IJ, Fletcher JM, James JB, Haugen TO, Vøllestad LA, Stenseth NC (2007) Trait changes in a harvested population are driven by a dynamic tug-of-war between natural and harvest selection. Proc Natl Acad Sci USA 104:15799–15804

Ernande B, Dieckmann U, Heino M (2004) Adaptive changes in harvested populations: plasticity and evolution of age and size at maturation. Proc Roy Soc Lond B 271:415–423

Folkvord A, Jørgensen C, Korsbrekke K, Nash RDM, Nilsen T, Skjæraasen JE (2014) Trade-offs between growth and reproduction in wild Atlantic cod. Can J Fish Aquat Sci 71:1106–1112

Gibbons JW, Semlitsch RD, Greene JL, Schubauer JP (1981) Variation in age and size at maturity of the slider turtle (*Pseudemys scripta*). Am Nat 117:841–845

Hairston NG Jr, Ellner SP, Geber MA, Yoshida T, Fox JA (2005) Rapid evolution and the convergence of ecological and evolutionary time. Ecol Lett 8:1114–1127

Kozłowski J (1992) Optimal allocation of resources to growth and reproduction: Implications for age and size at maturity. Trends Ecol Evol 7:15–19

Kozłowski J, Czarnoleski M, Danko M (2004) Can optimal resource allocation models explain why ectotherms grow larger in cold? Integr Comp Biol 44:480–493

Lande R (1977) On comparing coefficients of variation. Syst Zool 26:214–217

Lewontin RC (1965) Selection for colonizing ability. In: Baker H, Stebbins G (eds) The genetics of colonizing species. Academic, New York, pp 79–94

Luhring TM, Holdo RM (2015) Trade-offs between growth and maturation: the cost of reproduction for surviving environmental extremes. Oecologia 178:723–732

Perrin N (1995) About Berrigan and Charnov's life-history puzzle. Oikos 73:137–139

Phillips BL, Brown GP, Shine R (2010) Life-history evolution in range-shifting populations. Ecology 91:1617–1627

Post DM, Palkovacs EP (2009) Eco-evolutionary feedbacks in community and ecosystem ecology: interactions between the ecological theatre and the evolutionary play. Phil Trans Roy Soc Lond B 364:1629–1640

Reznick DA, Bryga H, Endler JA (1990) Experimentally induced life-history evolution in a natural population. Nature 346:357–359

Riessen HP (1999) Predator-induced life history shifts in *Daphnia*: a synthesis of studies using meta-analysis. Can J Fish Aquat Sci 56:2487–2494

Roff DA (1986) Predicting body size with life history models. Bioscience 36:316–323

Roff D (1993) Evolution of life histories: Theory and Analysis. Springer, New York

Rogerson A (1981) The ecological energetics of *Amoeba proteus* (Protozoa). Hydrobiologia 85:117–128

Rosenzweig ML, MacArthur RH (1963) Graphical representation and stability conditions of predator-prey interactions. Am Nat 97:209–223

Schoener TW (2011) The newest synthesis: understanding the interplay of evolutionary and ecological dynamics. Science 331:426–429

Stearns SC (1992) The evolution of life histories. Oxford University Press, USA

Stearns SC, Ackermann M, Doebeli M, Kaiser M (2000) Experimental evolution of aging, growth, and reproduction in fruitflies. Proc Natl Acad Sci USA 97:3309–3313

Turcotte MM, Reznick DN, Hare JD (2011) The impact of rapid evolution on population dynamics in the wild: experimental test of eco-evolutionary dynamics. Ecol Lett 14:1084–1092

von Bertalanffy L (1960) Principles and theory of growth. In: Nowinski WK (ed) Fundamental aspects of normal and malignant growth. Elsevier, New York, pp 137–259

Walsh MR, Reznick DN (2008) Interactions between the direct and indirect effects of predators determine life history evolution in a killifish. Proc Natl Acad Sci USA 105:594–599

Williams GC (1966) Natural selection, the costs of reproduction, and a refinement of Lack's principle. Am Nat 100:687–690

Wright S (1931) Evolution in Mendelian populations. Genetics 16:97–159

Wright S (1949) The genetical structure of populations. Ann Eugen 15:323–354

Yaari G, Ben-Zion Y, Shnerb NM, Vasseur DA (2012) Consistent scaling of persistence time in metapopulations. Ecology 93:1214–1227